MAGNETIC DOMAIN WALL MOTION
IN NANOSCALE MULTIFERROIC DEVICES
UNDER THE COMBINED ACTION OF MAGNETOSTRICTION,
RASHBA EFFECT AND DRY-FRICTION DISSIPATION

GIANCARLO CONSOLO[a] AND GIOVANNA VALENTI[b*]

ABSTRACT. The one-dimensional propagation of magnetic domain walls in a ferromagnetic nanostrip is investigated analytically in the framework of the extended Landau-Lifshitz-Gilbert equation. In particular, this study focuses on the characterization of the domain wall motion in the presence of stresses induced by a piezoelectric actuator, Rashba spin-orbit-torque due to structural inversion asymmetry and dry-friction dissipation accounting for structural disorder into the crystal lattice. By adopting the formalism of travelling waves and using realistic assumptions on the parameters here involved, it has been possible to deduce an explicit analytical expression of the DW velocity in the steady regime. It is also proven that the depinning threshold and the Walker breakdown, representing the boundaries of such a dynamical regime, are both affected by the strength of magnetostriction, Rashba field and dry-friction. Moreover, it is observed that the Rashba effect can also modify the domain wall mobility as well as the direction of propagation. The results here obtained are in qualitative good agreement with recent numerical simulations and experimental observations.

1. Introduction

Manipulation of the domain wall (DW) propagation in ferromagnetic nanostrips is nowadays attracting a lot of interest from both physical and technological viewpoints. Many efforts have been indeed made to exploit DW dynamics in several contexts such as sensors, logic gates, spin-wave filters and memories (Allwood 2005; Parkin *et al.* 2008; Weiler *et al.* 2009; Boulle *et al.* 2011).

The working principle behind any of these devices is typically the interaction among an electric current, a magnetic field and the magnetization state of single or multi-layer structures which gives rise to Spin-Transfer Torque (STT) and Spin-Orbit Torque (SOT) phenomena (Liu *et al.* 2011; Miron *et al.* 2011; Wang and Manchon 2012; Manchon *et al.* 2015; Pylypovskyi *et al.* 2016; Xu *et al.* 2016). The STT originates when a spin-polarized current crosses a DW and transfers its angular momentum to the internal structure of the DW, thereby pushing it along the direction of the current flow (Zhang and Li 2004; Thiaville

This paper is dedicated to the memory of Prof. Gaetano Giaquinta (1945–2016)

et al. 2005; Tatara *et al.* 2007; Koyama *et al.* 2011). The SOT has been observed in systems lacking of inversion symmetry where the electronic energy bands are split by spin-orbit coupling. In these structures, a charge current passing through a ferromagnet (or a bilayer ferromagnet/heavy metal) generates a non-equilibrium spin density via the inverse spin galvanic effect which is able to exert a torque on the local magnetization of the ferromagnet. The origin of SOT could be due to two phenomena: Rashba and spin-Hall effects. In particular, the exploration of Rashba coupling is nowadays drawing particular attention for the possibility to build up low-energy spintronic devices (Miron *et al.* 2011; Wang and Manchon 2012; Manchon *et al.* 2015; Pylypovskyi *et al.* 2016; Xu *et al.* 2016).

Besides these current-induced phenomena, it has been demonstrated that the position of a magnetic DW can be also manipulated via the magneto-elastic field. However, since the weak ferromagnetism at room temperature of natural multiferroics limits their applications, a strategy employed to achieve a significant magneto-electric coupling consists of exploiting the inverse magneto-electric effect by depositing or gluing a magnetic system onto a piezoelectric actuator. The heterostructure so obtained realizes a voltage controlled magnetic system where the strains generated by an electric field into the piezoelectric layer are efficiently transferred onto the ferromagnet (Liu *et al.* 2010; Bryan *et al.* 2012; Lei *et al.* 2013; Ranieri *et al.* 2013; Zighem *et al.* 2013; Brandl *et al.* 2014; Hu *et al.* 2016; Mathurin *et al.* 2016).

On the other hand, the characterization of realistic magnetic devices needs to account also for the damping effects arising from structural disorder such as inhomogeneities, impurities and crystallographic defects. These anisotropic dissipation mechanisms can be described by means of a rate-independent dry friction contribution (Baltensperger and Helman 1993; Podio-Guidugli and Tomassetti 2002; Tiberkevich and Slavin 2007; Consolo *et al.* 2012; Consolo and Valenti 2012, 2017).

The purpose of this work is to investigate analytically the DW dynamics obtained when all the above mentioned effects act together on a ferromagnetic nanostrip. As known, the magnetization dynamics occurring in such a system are well described by the Extended Landau-Lifshitz-Gilbert (ELLG) equation which characterizes the precessional motion of the magnetization vector about the direction of the effective field in the presence of concurrent dissipative phenomena: the intrinsic Gilbert damping torque and the current-induced spin-transfer-torque (Landau and Lifschitz 1935; Gilbert 1955; Schryer and Walker 1974; Berger 1984; Puliafito and Consolo 2012; Consolo *et al.* 2014a; Consolo *et al.* 2014b). In the present framework, the magneto-elastic effect enters the governing equation as an additive contribution to the effective field, the Rashba effect gives rise to a field-like term and a spin-torque-like term whereas the dry-friction dissipation is added to the Gilbert damping torque.

Owing to the complexity of the resulting ELLG equation, the solution is generally found via numerical simulations (Shu *et al.* 2004; Baňas 2008; Lei *et al.* 2013; Liang *et al.* 2014; Mballa-Mballa *et al.* 2014; Hu *et al.* 2016; Mathurin *et al.* 2016). Nevertheless, in this work, we aim to describe analytically the one-dimensional DW motion under the following assumptions: the magnetostrictive layer is isotropic; the piezoelectric-induced strains are spatially uniform and fully transferred into the ferromagnetic layer; the dry-friction coefficient depends linearly on the piezoelectric-induced strains and the Rashba SOT does not substantially modify the classical Walker solution. Let us emphasize that, in
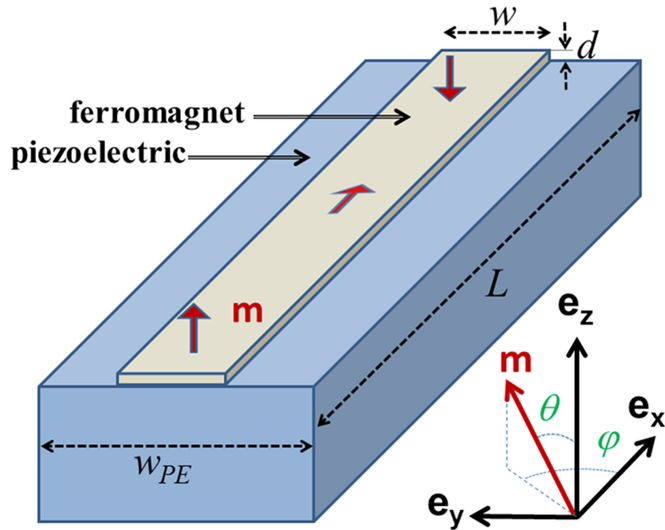
FIGURE 1. Schematics of the multiferroic device consisting of a thin magnetostrictive ferromagnetic nanostrip placed on the top of a thick piezoelectric layer.

spite of these simplifying assumptions, the resulting DW dynamics are still quite rich and in qualitative agreement with experimental observations.

The manuscript is organized as follows.

In Section **2** we build up a 1D model based upon the ELLG equation for the description of the DW motion in ferromagnetic nanostrips under the simultaneous influence of magnetic fields, spin-polarized currents, Rashba and magneto-elastic effects. In such a model, dissipation is account for by a standard linear Gilbert damping and a nonlinear dry-friction term. Then, the explicit analytical expression of the main characteristic parameters involved into the steady dynamical regime are derived by adopting a travelling wave ansatz.

In Section **3**, we use realistic values for the parameters in order to evaluate numerically the analytical results deduced in Section 2. In particular, we aim to elucidate the functional dependence of the characteristic parameters on the piezo-induced strains and the Rashba field as well as to quantify the role played by these contributions into the steady DW dynamics.

In Section **4**, we address some concluding remarks.

2. The mathematical 1D model

Let us consider a nanoscale multiferroic device composed by a thin magnetostrictive ferromagnet (FM) placed on the top surface of a thick piezoelectric (PE) actuator, as sketched in Fig. 1.

The FM layer is designed as a nanostrip of length L, width w and thickness d along $\mathbf{e_x}, \mathbf{e_y}, \mathbf{e_z}$ axes, respectively, with $L \gg w > d$. This layer is subject to an external bias

magnetic field $\mathbf{h}^{ext} = (h_x, h_y, h_z)$ and is traversed by an electric current density J flowing along the major axis $\mathbf{e}_x$. These driving sources are assumed to be constant in time and uniform in space. Two magnetic domains are nucleated at the edges of the FM layer and the resulting DW, which at equilibrium is located at the center of the structure, can be shifted along the nanostrip axis $\mathbf{e}_x$ via the external magnetic field and/or the electric current.

The PE layer serves as an actuator that deforms upon the application of an electric voltage imposed between two lateral electrodes. This voltage generates an electric field directed along the axis $\mathbf{e_y}$ which induces, in turn, an elongation or a compression of the PE width w_{PE} depending on the sign of the applied voltage. Owing to the elastic properties of the PE layer, the elongation (compression) along the $\mathbf{e_y}$ axis is accompanied by a compression (elongation) in the two orthogonal directions. However, since the PE thickness along the axis $\mathbf{e_z}$ is quite large, the corresponding strain component is usually neglected. For simplicity, all the shear strains are also disregarded . According to these assumptions, the only non-null planar strain components are $\varepsilon_{xx}^{(PE)}$ and $\varepsilon_{yy}^{(PE)}$ that are related to each other via the Poisson ratio ν (Weiler *et al.* 2009; Zighem *et al.* 2013).

The one-dimensional DW motion occurring at mesoscale in the FM layer can be described through the ELLG equation (Landau and Lifschitz 1935; Gilbert 1955; Schryer and Walker 1974; Berger 1984; Puliafito and Consolo 2012; Consolo *et al.* 2014a; Consolo *et al.* 2014b):

$$\dot{\mathbf{m}} = \mathbf{t}^{pre} + \mathbf{t}^{stt} + \mathbf{t}^{ra} + \mathbf{t}^{d} \tag{1}$$

where $\mathbf{m}(x,t) = \mathbf{M}(x,t)/M_S$ represents the normalized magnetization vector with M_S the saturation magnetization and the over-dot denotes the partial time derivative.

In detail, the first term $\mathbf{t}^{pre}$ on the right-hand side of (1) defines the undamped precessional torque induced by the effective magnetic field $\mathbf{h}^{eff}$ which, in turn, accounts for the contributions arising from external $\mathbf{h}^{ext}$, exchange $\mathbf{h}^{exc}$, demagnetizing $\mathbf{h}^{dmg}$ and magnetoelastic $\mathbf{h}^{mel}$ fields (Zhu *et al.* 2001; Zhang and Chen 2005):

$$\mathbf{t}^{pre} = \gamma \mathbf{h}^{eff} \wedge \mathbf{m} \tag{2a}$$

$$\mathbf{h}^{eff} = \mathbf{h}^{ext} + \mathbf{h}^{exc} + \mathbf{h}^{dmg} + \mathbf{h}^{mel} \tag{2b}$$

where $\gamma = M_S \mu_0 \gamma_e$ is a constant expressed in terms of the magnetic permeability of the vacuum μ_0 and of the gyromagnetic ratio $\gamma_e = ge/m_e$, being g the Landè factor, e the electron charge and m_e the electron mass.

The exchange field $\mathbf{h}^{exc}$ can be written as:

$$\mathbf{h}^{exc} = A \frac{\partial^2 \mathbf{m}}{\partial x^2} \tag{3}$$

being $A = \frac{2A_{ex}}{\mu_0 M_S^2}$ related to the exchange constant of the material A_{ex} through $A = \frac{2A_{ex}}{\mu_0 M_S^2}$.

The demagnetizing field $\mathbf{h}^{dmg}$ can be safely approximated by:

$$\mathbf{h}^{dmg} = -N_x (\mathbf{m} \cdot \mathbf{e}_x) \mathbf{e}_x - N_y (\mathbf{m} \cdot \mathbf{e}_y) \mathbf{e}_y - N_z (\mathbf{m} \cdot \mathbf{e}_z) \mathbf{e}_z \tag{4}$$

where the demagnetizing factors N_x, N_y, N_z are constrained by the normalization condition $N_x + N_y + N_z = 1$.

Moreover, if we consider the Hooke law as the linear constitutive assumption relating stress and strain in the FM, the magnetoelastic field $\mathbf{h}^{mel}$ reads:

$$\mathbf{h}^{mel} = \frac{1}{\mu_0 M_s^2} \mathbb{C} \left(\varepsilon - \varepsilon^\mu \right) \frac{\partial \varepsilon^\mu}{\partial \mathbf{m}} \tag{5}$$

where, in the case of an isotropic material, the elastic stiffness tensor $\mathbb{C}$ can be expressed as:

$$\mathbb{C} = \begin{bmatrix} c_{11} & c_{12} & c_{12} & & & \\ c_{12} & c_{11} & c_{12} & & \mathbf{0} & \\ c_{12} & c_{12} & c_{11} & & & \\ & & & \frac{c_{11}-c_{12}}{2} & 0 & 0 \\ & \mathbf{0} & & 0 & \frac{c_{11}-c_{12}}{2} & 0 \\ & & & 0 & 0 & \frac{c_{11}-c_{12}}{2} \end{bmatrix} \tag{6}$$

being c_{11} and c_{12} the two independent elastic constants in the Voigt notation.

In (5), ε and ε^μ denote the total strain tensor and the stress-free magnetostriction strain tensor, respectively, which are assumed to be spatially homogeneous. The magnetostriction strain tensor ε^μ is given by:

$$\varepsilon^\mu = \frac{3}{2} \lambda_S \left(\mathbf{m} \otimes \mathbf{m} - \frac{1}{3} \mathbf{I} \right), \tag{7}$$

λ_S being the saturation magnetostriction constant, $\mathbf{I}$ the identity tensor and the symbol $\otimes$ representative of the tensor product. About the total strain tensor ε, it can be hypothesized that, since the FM layer is affixed to the top xy face of the PE actuator, the planar strains $\varepsilon_{xx}^{(PE)}$ and $\varepsilon_{yy}^{(PE)}$ are fully transferred from the PE to the FM, namely $\varepsilon_{xx} = \varepsilon_{xx}^{(PE)}$ and $\varepsilon_{yy} = \varepsilon_{yy}^{(PE)}$. Moreover, owing to the small thickness of the FM layer, its free upper surface and the negligible shear strain in the plane xy, it is also reasonable to assume that the FM layer is in a plane bitension stress state characterized by (Lei *et al.* 2013; Hu *et al.* 2016; Mathurin *et al.* 2016):

$$\varepsilon_{xy} = \varepsilon_{xz} = \varepsilon_{yz} = 0, \tag{8a}$$

$$\varepsilon_{zz} = -\frac{c_{12}}{c_{11}} \left(\varepsilon_{xx} + \varepsilon_{yy} \right) = -\frac{c_{12}}{c_{11}} \left(1 - v \right) \varepsilon_{yy}. \tag{8b}$$

The second torque term $\mathbf{t}^{stt}$ appearing in (1) accounts for the spin-transfer torque generated by the current flow and includes the adiabatic and non-adiabatic contributions responsible for the DW distortion and motion, respectively (Zhang and Li 2004; Thiaville *et al.* 2005). It reads:

$$\mathbf{t}^{stt} = u_0 \left[-\frac{\partial \mathbf{m}}{\partial x} - \eta \frac{\partial \mathbf{m}}{\partial x} \wedge \mathbf{m} \right] J \tag{9}$$

with η the phenomenological non-adiabatic parameter and $u_0 = g\mu_B P / (2eM_s)$, being μ_B the Bohr magneton and P the polarization factor of the current.

The third term $\mathbf{t}^{ra}$ in (1) describes the current-induced Rashba effect that enters the governing equation both as a field-like term and as a spin-transfer-torque-like term. In fact, it is given by:

$$\mathbf{t}^{ra} = \gamma \widehat{\alpha}_{ra} \left[\mathbf{e_y} \wedge \mathbf{m} + \eta \mathbf{m} \wedge \left(\mathbf{m} \wedge \mathbf{e_y} \right) \right] J \tag{10}$$

being $\widehat{\alpha}_{ra} = \frac{\alpha_R P}{\mu_0 \mu_B M_S^2}$ with α_R the parameter that measures the strength of the Rashba spin-orbit-torque.

Finally, the torque term $\mathbf{t}^d$ in (1), accounting for the intrinsic dissipative phenomena, includes the classical Gilbert damping torque (Gilbert 1955) augmented by a non linear contribution arising from a rate-independent dry friction (Baltensperger and Helman 1993; Podio-Guidugli and Tomassetti 2002; Tiberkevich and Slavin 2007; Consolo *et al.* 2012; Consolo and Valenti 2012, 2017), namely:

$$\mathbf{t}^d = \alpha_G \left(\mathbf{m} \wedge \dot{\mathbf{m}} \right) + \mathbf{m} \wedge \left(\gamma \alpha_D |\dot{\mathbf{m}}|^{-1} \dot{\mathbf{m}} \right) \tag{11}$$

The phenomenological dimensionless parameters α_G and α_D describe the strength of linear and nonlinear dissipation, respectively. As known from literature, the dry-friction term can mimic the pinning effects due to the presence of crystallographic defects or inhomogeneities into the FM layer. Moreover, this term can also account, at least in principle, for the magnification of such pinning effects caused by the piezo-induced stress. Therefore, it is reasonable to assume that the dry-friction coefficient depends upon the piezo-strain, $\alpha_D = \alpha_D(\varepsilon_{yy})$, as conjectured in our previous work (Consolo and Valenti 2017).

To analytically gain insight into DW dynamics, we substitute the explicit expressions of the above defined torques into the ELLG equation (1) which, in polar coordinates, becomes:

$$
\begin{aligned}
&\sin\theta\, \dot{\varphi} - \left[\alpha_G + \gamma\alpha_D \left(\dot{\theta}^2 + \sin^2\theta\, \dot{\varphi}^2 \right)^{-1/2} \right] \dot{\theta} \\
&= \gamma \Bigg\{ -A\frac{\partial^2\theta}{\partial x^2} + A\sin\theta\cos\theta \left(\frac{\partial\varphi}{\partial x} \right)^2 - h_x\cos\theta\cos\varphi - h_y\cos\theta\sin\varphi + h_z\sin\theta \\
&\quad + \Bigg[N_x\cos^2\varphi + N_y\sin^2\varphi - N_z \\
&\quad - \frac{3\lambda_S}{\mu_0 M_s^2}\frac{c_{11}-c_{12}}{c_{11}} \left[c_{11}\left(\varepsilon_{xx}\cos^2\varphi + \varepsilon_{yy}\sin^2\varphi \right) + c_{12}\left(\varepsilon_{xx}+\varepsilon_{yy} \right) \right] \Bigg] \sin\theta\cos\theta \\
&\quad - \widehat{\alpha}_{ra}J\cos\theta\sin\varphi - \eta\widehat{\alpha}_{ra}J\cos\varphi \Bigg\} - u_0 J\sin\theta\frac{\partial\varphi}{\partial x} + \eta u_0 J\frac{\partial\theta}{\partial x}\,,
\end{aligned}
\tag{12a}
$$

$$
\begin{aligned}
&\left[\alpha_G + \gamma\alpha_D \left(\dot{\theta}^2 + \sin^2\theta\, \dot{\varphi}^2 \right)^{-1/2} \right] \sin\theta\, \dot{\varphi} + \dot{\theta} \\
&= \gamma \Bigg\{ A\sin\theta\frac{\partial^2\varphi}{\partial x^2} + 2A\cos\theta\frac{\partial\theta}{\partial x}\frac{\partial\varphi}{\partial x} + h_y\cos\varphi - h_x\sin\varphi \\
&\quad + \left[N_x - N_y + \frac{3\lambda_S}{\mu_0 M_s^2}\left(c_{11}-c_{12} \right)\left(\varepsilon_{yy}-\varepsilon_{xx} \right) \right] \sin\theta\cos\varphi\sin\varphi - \eta\widehat{\alpha}_{ra}J\cos\theta\sin\varphi \Bigg\} \\
&\quad - \eta u_0 J\sin\theta\frac{\partial\varphi}{\partial x} - u_0 J\frac{\partial\theta}{\partial x}\,,
\end{aligned}
\tag{12b}
$$

where θ and φ are the polar and azimuthal angles, respectively, so that the unit magnetization vector $\mathbf{m}$ can be expressed as $\mathbf{m} = (\cos\varphi\sin\theta, \sin\varphi\sin\theta, \cos\theta)$.

In order to describe the dynamical regime characterized by a steady motion of the DW along the nanostrip axis $\mathbf{e}_x$ with constant velocity v, let us introduce the travelling wave

ansatz for the polar angle $\theta = \theta(x - vt)$ whereas the azimuthal angle is assumed to be constant in time and uniform in space $\varphi = \varphi_0$ (Schryer and Walker 1974).

Under these assumptions, the system (12) reduces to:

$$[\alpha_G v - \eta u_0 J]\, \theta' + \widehat{\alpha_D} = \gamma \Big\{ -A\theta'' - h_x \cos\theta \cos\varphi_0 - h_y \cos\theta \sin\varphi_0 + h_z \sin\theta$$

$$- \widehat{\alpha}_{ra} J \cos\theta \sin\varphi_0 - \eta \widehat{\alpha}_{ra} J \cos\varphi_0 + \sin\theta \cos\theta \Big[N_x \cos^2\varphi_0 + N_y \sin^2\varphi_0 - N_z$$

$$- \frac{3\lambda_S}{\mu_0 M_s^2}\, \frac{(c_{11} - c_{12})}{c_{11}} \Big[c_{11}\left(\varepsilon_{xx}\cos^2\varphi_0 + \varepsilon_{yy}\sin^2\varphi_0\right) + c_{12}\left(\varepsilon_{xx} + \varepsilon_{yy}\right) \Big] \Big] \Big\}, \qquad (13a)$$

$$(u_0 J - v)\,\theta' = \gamma \Big\{ h_y \cos\varphi_0 - h_x \sin\varphi_0 + \widehat{\alpha}_{ra} J \cos\varphi_0 - \eta \widehat{\alpha}_{ra} J \cos\theta \sin\varphi_0$$

$$+ \Big[(N_x - N_y) + \frac{3\lambda_S}{\mu_0 M_s^2}(c_{11} - c_{12})(\varepsilon_{yy} - \varepsilon_{xx}) \Big] \sin\theta \cos\varphi_0 \sin\varphi_0 \Big\}, \qquad (13b)$$

where the prime denotes the derivative with respect to the travelling wave variable $\xi = x - vt$ and $\widehat{\alpha_D} = \gamma \alpha_D \mathrm{sign}(v\theta')$.

It is straightforward to see that eq. (13b) can be recast as:

$$\theta' = \Gamma\left(\sin\theta + \widetilde{\Gamma}\cos\theta + \widehat{\Gamma}\right) \qquad (14)$$

with:

$$\Gamma = \frac{\gamma}{u_0 J - v}\left[\frac{N_x - N_y}{2} + \frac{3\lambda_S}{2\mu_0 M_s^2}(c_{11} - c_{12})(\varepsilon_{yy} - \varepsilon_{xx}) \right]\sin 2\varphi_0, \qquad (15a)$$

$$\widetilde{\Gamma} = -\frac{\eta \widehat{\alpha}_{ra}}{\left[N_x - N_y + \frac{3\lambda_S}{\mu_0 M_s^2}(c_{11} - c_{12})(\varepsilon_{yy} - \varepsilon_{xx}) \right]\cos\varphi_0}\, J = -\widetilde{\Gamma}_1 J, \qquad (15b)$$

$$\widehat{\Gamma} = \frac{h_y \cos\varphi_0 - h_x \sin\varphi_0 + \widehat{\alpha}_{ra}\cos\varphi_0 J}{\left[N_x - N_y + \frac{3\lambda_S}{\mu_0 M_s^2}(c_{11} - c_{12})(\varepsilon_{yy} - \varepsilon_{xx}) \right]\sin\varphi_0 \cos\varphi_0} = \widehat{\Gamma}_0 + \widehat{\Gamma}_1 J, \qquad (15c)$$

where Γ^{-1} has the dimension of length while $\widetilde{\Gamma}$ and $\widehat{\Gamma}$ are dimensionless parameters.

Then, inserting (14) into (13a), after some algebra, leads to:

$$P\sin\theta + Q\cos\theta + R\sin\theta\cos\theta + S\sin^2\theta + T = 0 \qquad (16)$$

where:

$$P = \Gamma(\alpha_G v - \eta u_0 J) - \gamma\left(h_z + A\Gamma^2 \widehat{\Gamma}\widetilde{\Gamma}\right), \qquad (17a)$$

$$Q = \Gamma\widetilde{\Gamma}(\alpha_G v - \eta u_0 J) + \gamma\left(h_x \cos\varphi_0 + h_y \sin\varphi_0 + A\Gamma^2\widehat{\Gamma} + \widehat{\alpha}_{ra} J \sin\varphi_0 \right), \qquad (17b)$$

$$R = \gamma\Big\{ A\Gamma^2\left(1 - \widetilde{\Gamma}^2\right) + N_z - N_y\sin^2\varphi_0 - N_x\cos^2\varphi_0$$

$$+ \frac{3\lambda_S}{\mu_0 M_s^2}\left(\frac{c_{11} - c_{12}}{c_{11}}\right)\Big[c_{11}\left(\varepsilon_{xx}\cos^2\varphi_0 + \varepsilon_{yy}\sin^2\varphi_0\right) + c_{12}\left(\varepsilon_{xx} + \varepsilon_{yy}\right) \Big] \Big\}, \qquad (17c)$$

$$S = -2\gamma A \Gamma^2 \widetilde{\Gamma}, \tag{17d}$$

$$T = \Gamma\widehat{\Gamma}\left(\alpha_G v - \eta u_0 J\right) + \widehat{\alpha_D} + \gamma\left(A\Gamma^2\widetilde{\Gamma} + \eta\widehat{\alpha}_{ra}J\cos\varphi_0\right). \tag{17e}$$

Furthermore, taking into account some previous results (Consolo *et al.* 2012; Consolo and Valenti 2012, 2017), the expression of the DW width $\delta = \Gamma^{-1}$ can be deduced from (17c) by imposing $R = 0$. Thus, we have:

$$\delta^{-2} = \Gamma^2 = \frac{1}{A\left(1 - \widetilde{\Gamma}^2\right)}\left\{ N_x\cos^2\varphi_0 + N_y\sin^2\varphi_0 - N_z \right.$$

$$\left. - \frac{3\lambda_S}{\mu_0 M_s^2}\frac{(c_{11} - c_{12})}{c_{11}}\left[c_{11}\left(\varepsilon_{xx}\cos^2\varphi_0 + \varepsilon_{yy}\sin^2\varphi_0\right) + c_{12}\left(\varepsilon_{xx} + \varepsilon_{yy}\right)\right] \right\}. \tag{18}$$

Comparing (18) with the expression found in (Consolo and Valenti 2017), we notice that the presence of the Rashba field reduces, via the coefficient $\widetilde{\Gamma}$, the DW width.

As it can be proven, a meaningful solution of eq. (14) satisfying the symmetry condition $\theta(0) = \pi/2$ is admitted for $\left|\widehat{\Gamma}^2 - \widetilde{\Gamma}^2\right| < 1$ only and it can be expressed as (Podio-Guidugli and Tomassetti 2002; Consolo and Valenti 2012, 2017):

$$\theta(\xi) = 2\arctan\frac{Fk_2\exp\left(\Gamma\sqrt{1 + \widetilde{\Gamma}^2 - \widehat{\Gamma}^2}\xi\right) - k_1}{F\exp\left(\Gamma\sqrt{1 + \widetilde{\Gamma}^2 - \widehat{\Gamma}^2}\xi\right) - 1} \tag{19}$$

with:

$$F = \frac{1 + \left(\widehat{\Gamma} - \widetilde{\Gamma}\right)\left(1 - \widetilde{\Gamma}\right) - \left(\widehat{\Gamma} - \widetilde{\Gamma} + 1\right)\sqrt{1 + \widetilde{\Gamma}^2 - \widehat{\Gamma}^2}}{\left(\widehat{\Gamma} - \widetilde{\Gamma}\right)\left(\widehat{\Gamma} + 1\right)}, \tag{20a}$$

$$k_1 = \frac{-1 + \sqrt{1 + \widetilde{\Gamma}^2 - \widehat{\Gamma}^2}}{\widehat{\Gamma} - \widetilde{\Gamma}}, \tag{20b}$$

$$k_2 = \frac{-1 - \sqrt{1 + \widetilde{\Gamma}^2 - \widehat{\Gamma}^2}}{\widehat{\Gamma} - \widetilde{\Gamma}}. \tag{20c}$$

Remark 1. Let us point out that, in the limit $\left|\widetilde{\Gamma}\right| \to 0, \left|\widehat{\Gamma}\right| \to 0$, we obtain the classical Walker solution representing a 180° Bloch DW with $\theta(\xi) \simeq \pi$ for $\xi \to +\infty$ and $\theta(\xi) \simeq 0$ for $\xi \to -\infty$ (Schryer and Walker 1974). On the other hand, from (14) it is easy to see that, when $\left|\widetilde{\Gamma}\right|$ and $\left|\widehat{\Gamma}\right|$ increase, the magnetic domains at the boundaries of the nanostrip are not anymore aligned with the $\mathbf{e}_z$ axis so that the solution deviates away from the classical one. Therefore, without loss of generality, hereafter we limit our discussion to the cases $\left|\widetilde{\Gamma}\right| \simeq 0, \left|\widehat{\Gamma}\right| \simeq 0$ that can be easily achieved by using realistic values for the parameters. Consequently, the DW width (18) exhibits a weak dependence on the Rashba field as well as on the piezo-strains as it was proven in our previous work (Consolo and Valenti 2017). For this reason, the DW width $\delta = \Gamma^{-1}$ is treated as a constant, as usual in literature.

Under the above mentioned hypothesis, taking into account that the coefficients P, Q, T (see (17a), (17b), and (17e)) do not depend on θ, and averaging the equation (16) over

the range $0 \leq \theta \leq \pi$, the following expression of the DW velocity in the steady regime is obtained:

$$
v = \frac{1}{\alpha_G \Gamma \left(2 + \pi \widehat{\Gamma}_0 + \pi \widehat{\Gamma}_1 J \right)} \left\{ 2\gamma h_z + \left[u_0 \Gamma \eta \left(2 + \pi \widehat{\Gamma}_0 \right) - \eta \gamma \pi \widehat{\alpha}_{ra} \cos \varphi_0 - 2\gamma A \Gamma^2 \widehat{\Gamma}_0 \widetilde{\Gamma}_1 \right] J \right.
$$
$$
\left. + \widehat{\Gamma}_1 \Gamma \left(\eta \pi u_0 - 2\gamma A \Gamma \widetilde{\Gamma}_1 \right) J^2 - \pi \widehat{\alpha}_D \right\}.
\tag{21}
$$

In order to investigate how each driving source affects the DW velocity, let us now characterize the dynamics obtained when the magnetic field $\mathbf{h}^{ext}$ and the electric current J act separately.

In the absence of electric current, the DW velocity exhibits the expected linear dependence on the z-component of the magnetic field responsible for the DW motion, being the Rashba effect null (Consolo and Valenti 2017).

On the contrary, in the absence of external magnetic field, the presence of the Rashba field makes the coefficient $\widehat{\Gamma}_1 \neq 0$ so that the dependence of velocity on electric current becomes nonlinear. Moreover, taking into account (15b)-(15c), the Rashba field also affects the modulus and the sign of the DW mobility. In particular, at the critical value $\widehat{\alpha}_{ra} = \widehat{\alpha}_{ra}^*$ given by:

$$
\widehat{\alpha}_{ra}^* = \frac{\pi u_0 \left[N_x - N_y + \frac{3\lambda_S}{\mu_0 M_s^2} (c_{11} - c_{12}) (\varepsilon_{yy} - \varepsilon_{xx}) \right] \cos \varphi_0}{2\gamma A \Gamma}
\tag{22}
$$

the DW reverses its direction of motion so that a forward (backward) propagating DW is observed for $\widehat{\alpha}_{ra} < \widehat{\alpha}_{ra}^*$ ($\widehat{\alpha}_{ra} > \widehat{\alpha}_{ra}^*$). Let us also point out that the reversal of the propagation direction also affects the parameter $\widehat{\alpha}_D$, while the travelling profile $\theta(\xi)$ is unchanged.

As known, the steady dynamical regime can only take place in a well defined range of the external sources. The lower bound of such a range, named depinning threshold, corresponds to the minimum value of the magnetic field/electric current necessary to overcome the static friction. From eq. (21), it can be expressed as:

$$
J = 0 \Longrightarrow h_z^{(DEP)} = \frac{\pi}{2\gamma} \widehat{\alpha}_D,
\tag{23a}
$$
$$
\mathbf{h}^{ext} = \mathbf{0} \Longrightarrow \text{ for } \widehat{\alpha}_{ra} \lessgtr \widehat{\alpha}_{ra}^*,
$$
$$
J^{(DEP)} = \frac{1}{2\widehat{\Gamma}_1 \Gamma \left(\eta \pi u_0 - 2\gamma A \Gamma \widetilde{\Gamma}_1 \right)} \left\{ \eta \left(\gamma \pi \widehat{\alpha}_{ra} \cos \varphi_0 - 2u_0 \Gamma \right) \right.
$$
$$
\left. \pm \sqrt{\eta^2 \left(\gamma \pi \widehat{\alpha}_{ra} \cos \varphi_0 - 2u_0 \Gamma \right)^2 + 4\pi \widehat{\alpha}_D \widehat{\Gamma}_1 \Gamma \left(\eta \pi u_0 - 2\gamma A \Gamma \widetilde{\Gamma}_1 \right)} \right\}.
\tag{23b}
$$

As it can be observed, in the case of magnetic-field-driven motion, the nonlinear dry dissipation provides the only contribution to the depinning threshold. On the contrary, for a current-driven motion, such a threshold is also affected by Rashba field and piezo-induced strains, irrespective of the existence of a functional dependence between strain and dry-friction.

The upper bound of the steady motion range, named Walker Breakdown (WB), is deduced from (15a) and leads to the following restrictions to the DW velocity:

$$J = 0 \Longrightarrow v \leq \widetilde{v} \tag{24a}$$

$$\mathbf{h}^{ext} = \mathbf{0} \Longrightarrow \begin{cases} v \leq u_0 J + \widetilde{v} & \text{for } \widehat{\alpha}_{ra} < \widehat{\alpha}_{ra}^* \\ v \geq u_0 J - \widetilde{v} & \text{for } \widehat{\alpha}_{ra} > \widehat{\alpha}_{ra}^* \end{cases} \tag{24b}$$

$$\widetilde{v} = \frac{\gamma}{2\Gamma} \left| N_x - N_y + \frac{3\lambda_S}{\mu_0 M_s^2} (c_{11} - c_{12})(\varepsilon_{yy} - \varepsilon_{xx}) \right| \tag{24c}$$

Therefore, by comparing (21) with (24a) and (24b), we deduce the WB values for external field and current density:

$$h_z^{(WB)} = \frac{\pi}{2\gamma} \widehat{\alpha}_D + \frac{\alpha_G \Gamma \left(2 + \pi\widehat{\Gamma}_0 \right) \widetilde{v}}{2\gamma}, \tag{25a}$$

for $\widehat{\alpha}_{ra} < \widehat{\alpha}_{ra}^* \quad \Rightarrow$

$$
J_{upper}^{(WB)} = \frac{1}{2\widehat{\Gamma}_1 \Gamma \left[\pi u_0 (\eta - \alpha_G) - 2\gamma A\Gamma\widetilde{\Gamma}_1 \right]} \Bigg\{ 2u_0 \Gamma(\alpha_G - \eta) + \eta\gamma\pi\widehat{\alpha}_{ra}\cos\varphi_0 + \pi\alpha_G\widehat{\Gamma}_1\Gamma\widetilde{v}
$$
$$
+ \left[\left(2u_0\Gamma(\alpha_G - \eta) + \eta\gamma\pi\widehat{\alpha}_{ra}\cos\varphi_0 + \pi\alpha_G\widehat{\Gamma}_1\Gamma\widetilde{v} \right)^2 \right.
$$
$$
\left. + 4\widehat{\Gamma}_1\Gamma(\pi\widehat{\alpha}_D + 2\alpha_G\Gamma\widetilde{v}) \left(\pi u_0(\eta - \alpha_G) - 2\gamma A\Gamma\widetilde{\Gamma}_1 \right) \right]^{1/2} \Bigg\}, \tag{25b}
$$

for $\widehat{\alpha}_{ra} > \widehat{\alpha}_{ra}^* \quad \Rightarrow$

$$
J_{lower}^{WB} = \frac{1}{2\widehat{\Gamma}_1 \Gamma \left[\pi u_0 (\eta - \alpha_G) - 2\gamma A\Gamma\widetilde{\Gamma}_1 \right]} \Bigg\{ 2u_0 \Gamma(\alpha_G - \eta) + \eta\gamma\pi\widehat{\alpha}_{ra}\cos\varphi_0 - \pi\alpha_G\widehat{\Gamma}_1\Gamma\widetilde{v}
$$
$$
- \left[\left(2u_0\Gamma(\alpha_G - \eta) + \eta\gamma\pi\widehat{\alpha}_{ra}\cos\varphi_0 - \pi\alpha_G\widehat{\Gamma}_1\Gamma\widetilde{v} \right)^2 \right.
$$
$$
\left. + 4\widehat{\Gamma}_1\Gamma(\pi\widehat{\alpha}_D - 2\alpha_G\Gamma\widetilde{v}) \left(\pi u_0(\eta - \alpha_G) - 2\gamma A\Gamma\widetilde{\Gamma}_1 \right) \right]^{1/2} \Bigg\}. \tag{25c}
$$

Summarizing, a steady motion can only originate if the strength of the external source is greater than the propagation threshold (23) but smaller than the WB limit (25a), (25b). In particular, the maximum value of the electric current which allows a steady motion is given by $J_{upper}^{(WB)}$ or $J_{lower}^{(WB)}$, depending on the direction of propagation.

Let us finally notice that, since depinning threshold and WB conditions are both affected by Rashba, magnetoelastic and dry-friction, the whole steady dynamical regime can be modulated via current-induced spin-orbit-torque effects and/or via applied stresses, in accordance with experimental observations (Miron *et al.* 2011; Ranieri *et al.* 2013).

3. Numerical results

In order to estimate quantitatively the physical quantities introduced in the previous Section, we now present a numerical illustrative example by using realistic parameters extracted from literature.

About the PE layer, we consider that the in-plane strain difference $\left| \varepsilon_{yy}^{(PE)} - \varepsilon_{xx}^{(PE)} \right| = \left| \varepsilon_{yy} - \varepsilon_{xx} \right|$ lies in the range $\left[0, 10^{-3} \right]$ whereas the Poisson ratio is equal to $\nu = 0.39$ (Lei *et al.* 2013; Zighem *et al.* 2013; Mathurin *et al.* 2016).

About the FM material, we consider a metallic ferromagnetic nanostrip having length $L = 20 \ \mu m$, width $w = 160$ nm and thickness $d = 1$ nm so that the constraint $L >> w > d$ is satisfied. The set of parameters includes: saturation magnetization $M_S = 1 \times 10^6$ A/m, exchange constant $A_{ex} = 1 \times 10^{-11}$ J/m, dimensionless Gilbert damping constant $\alpha_G = 0.1$, demagnetizing factors $N_x = 0.8011$, $N_y = 0.0011$ and $N_z = 0.1978$, current polarization factor $P = 0.5$, non-adiabatic coefficient $\eta = 0.4$, elastic constants $c_{11} = 237$ GPa and $c_{12} = 117$ GPa, saturation magnetostriction $\lambda_S = 20$ ppm (Chen *et al.* 2002; Yamanouchi *et al.* 2011; Lei *et al.* 2013), $\varphi_0 = 10°$ and the Rashba parameter α_R lies in the range $[0, 2.0] \times 10^{-30}$ Jm. According to this set of parameters, the DW width is $\delta = \Gamma^{-1} \approx 5 nm$.

Moreover, since the aim of this work is to emphasize the role of the current-induced STT and SOT effects, the external magnetic field $\mathbf{h}^{ext}$ is neglected. On the other hand, DW dynamics driven by the sole magnetic field have been already investigated in a previous work (Consolo and Valenti 2017).

Let us firstly analyze the piezo-strain dependence of the dimensionless parameters $\widetilde{\Gamma}$ and $\widehat{\Gamma}$, defined in (15b)-(15c), which are strictly related to Rashba and magnetoelastic effects. As shown in Fig. 2, these quantities exhibit a weak dependence on the in-plane strain difference $\varepsilon_{yy} - \varepsilon_{xx}$ and their values satisfy the required constraints $\left| \widehat{\Gamma}^2 - \widetilde{\Gamma}^2 \right| < 1$ and $\left| \widetilde{\Gamma} \right|, \left| \widehat{\Gamma} \right| \simeq 0$.

We now investigate the traveling wave profile (19) obtained by using the values of $\widetilde{\Gamma}$ and $\widehat{\Gamma}$ reported in Fig. 2. As shown in Fig. 3, being $\theta(-\infty) \approx 0$ and $\theta(+\infty) \approx \pi$, the solution approximates quite well the Walker profile, so that we can safely treat it as a classical 180° Bloch DW.

To quantify the extreme of the interval in which the steady dynamical regime takes place, in agreement with our previous conjecture (Consolo and Valenti 2017), we assume a linear dependence of the dry-friction coefficient on the in-plane strain difference, namely:

$$\widehat{\alpha_D} = \gamma \left[\widehat{\alpha_0} + \widehat{\alpha_1} \left(\varepsilon_{yy} - \varepsilon_{xx} \right) \right] sign \left(v \theta' \right) \qquad (26)$$

where $\widehat{\alpha_0}$ and $\widehat{\alpha_1}$ are arbitrary constants. In particular, the first term measures the structural disorder resulting from the fabrication process of the FM material whereas the second one mimics the amplification of such disorder due to piezo-strains.

In order to evaluate the lower bound of the steady regime, in Fig.4 we represent the depinning current density $J^{(DEP)}$ as a function of the piezo-strain for several values of the Rashba parameter satisfying $\widehat{\alpha}_{ra} < \widehat{\alpha}_{ra}^*$. From this figure we notice that the depinning current is shifted upwards with the increase of both Rashba field and piezo-strains. These fields thus contribute in amplifying the pinning effects that prevent the DW from moving (Tatara *et al.* 2006).
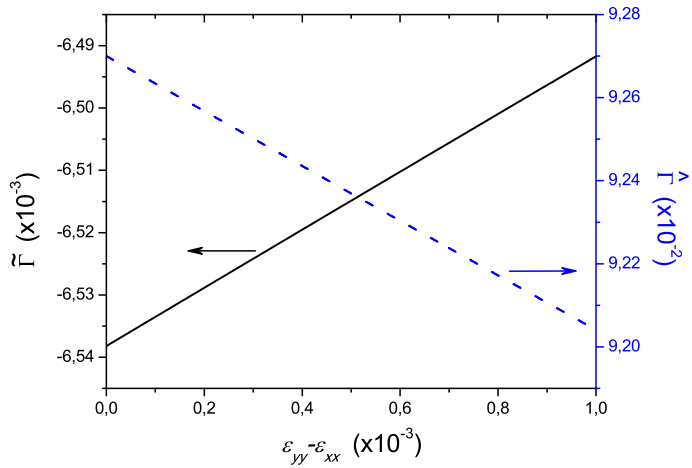
FIGURE 2. In-plane strain difference dependence of the parameters $\widetilde{\Gamma}$ (solid line) and $\widehat{\Gamma}$ (dashed line). The parameters used are: $\alpha_R = 0.3 \times 10^{-30}$ Jm and $J = 1$ $A/\mu m^2$.
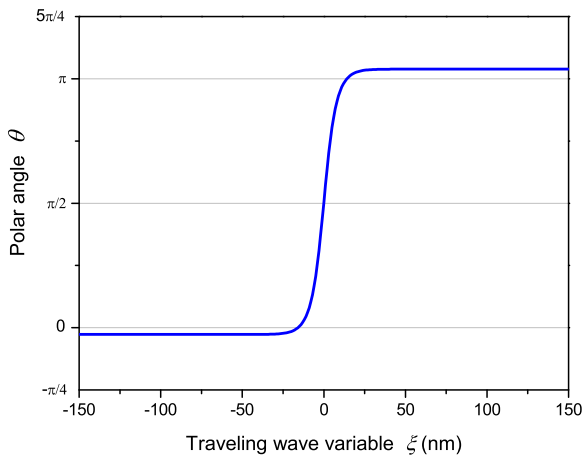

FIGURE 3. Traveling wave profile obtained by using the values of $\widetilde{\Gamma}$ and $\widehat{\Gamma}$ reported in Fig. 2

    The upper limit to the forward steady motion, given by the Walker Breakdown condition $J_{upper}^{(WB)}$, is represented in Fig.5. Results indicate that the Rashba field and the piezo-strains extend the steady regime towards larger values of the input current, allowing in turn the
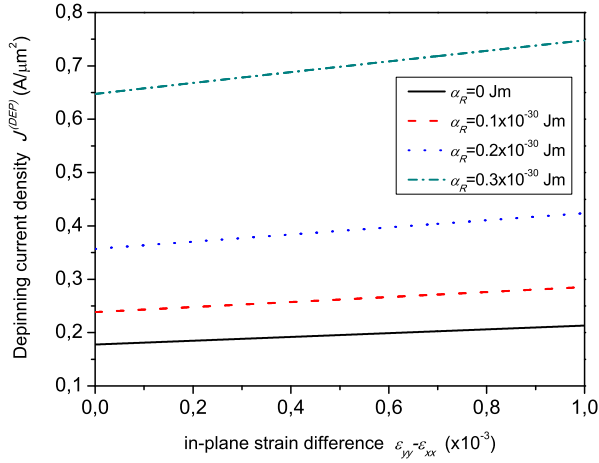
FIGURE 4. In-plane strain difference $\varepsilon_{yy} - \varepsilon_{xx}$ dependence of depinning current density $J^{(DEP)}$ for different values of the Rashba parameter α_R. The parameters here involved are: $J = 1 \, A/\mu m^2$, $\widehat{\gamma \alpha_0} = 2.5 \times 10^8 \, s^{-1}$ and $\widehat{\gamma \alpha_1} = 5 \times 10^{10} \, s^{-1}$.

DW velocity to achieve larger values. However, the shift of the WB condition appears to be much more dependent upon the strength of the Rashba field rather than the magnetoelastic one. For instance, if $\alpha_R = 0.3 \times 10^{-30} Jm$, the WB limit is about 3 times larger than the one obtained in the absence of Rashba contribution whereas it varies by less than 1% in the whole range of piezo-strains.

    We now inspect the dependence of the steady DW velocity obtained by fixing the piezo-strains and varying the Rashba contribution (see Fig.6a) and vice versa (see Fig.6b). In detail, from a direct inspection of Fig.6a we notice that the Rashba field affects the depinning threshold, the DW mobility and the direction of motion. In fact, in the regime of forward propagation ($v \geq 0$) and for a fixed value of electric current, the increase of the Rashba field leads to a reduction of the DW mobility. On the other hand, a greater Rashba field allows to achieve larger values of the steady DW velocity, being the corresponding upper WB limit shifted upward.

    If the Rashba parameter overcomes the critical value $\widehat{\alpha}_{ra}^*$ (corresponding to $\alpha_R = 1.25 \times 10^{-30} Jm$), the DW mobility changes sign and the direction of propagation is consequently reversed. In this case, the upper bound of the steady regime is given by $J_{lower}^{(WB)}$. As a consequence of that, the increase of the Rashba parameter leads now to an increase of the DW mobility and larger DW velocities (in absolute value) can be achieved by applying smaller current values.

    Finally, the investigation carried out by fixing the Rashba parameter and varying the in-plane piezo-strains (see Fig.6b) allows to conclude that the piezo-strains don't play any significant role in determining the DW mobility but they shift the DW motion towards
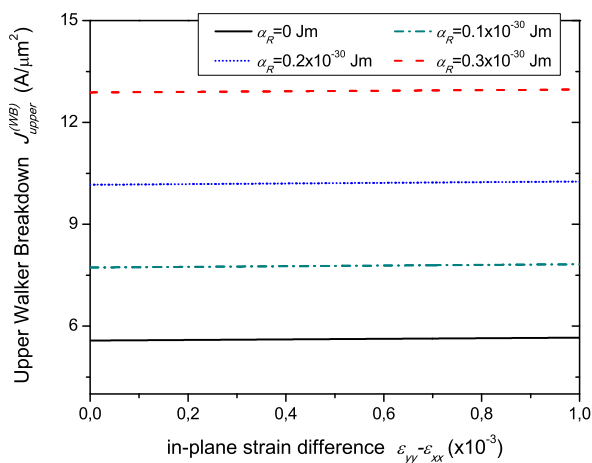
FIGURE 5. In-plane strain difference $\varepsilon_{yy} - \varepsilon_{xx}$ dependence of the upper Walker breakdown current density $J_{upper}^{(WB)}$ for different values of the Rashba parameter α_R. The parameters are the same as the ones used in Fig. 4

larger values of the input stimulus, as expected from the working principle behind a friction mechanism.

It is worthy noticing that our results are in qualitative good agreement with both numerical (Martinez and Finocchio 2013) and laboratory observations (Miron *et al.* 2011; Ranieri *et al.* 2013).

Remark 2. The analytical results presented in the previous Section describe the steady DW dynamics observed in metal or semiconductor ferromagnets. The numerical results shown in this Section depict the behavior of a metallic ferromagnet but can be used, at qualitative level, for a semiconductor as well. The most remarkable difference between them is that, since a semiconductor has typically a much smaller saturation magnetization value, it exhibits a significantly larger sensitivity of the characteristic parameters on the applied stresses. A quantitative comparison on the piezo-induced strain dependence of depinning threshold and Walker breakdown field/current for these materials can be found in Consolo and Valenti (2017).

4. Conclusions

In this work, the one-dimensional motion of magnetic DW driven by the simultaneous action of external magnetic field, spin-polarized current, Rashba effect and magnetostriction has been theoretically described in a bilayer piezoelectric/magnetostrictive nanostructure exhibiting crystallographic defects.

This study has been carried out by assuming that the FM material is isotropic; the biaxial in-plane strains are spatially uniform and fully transferred from the PE actuator to the
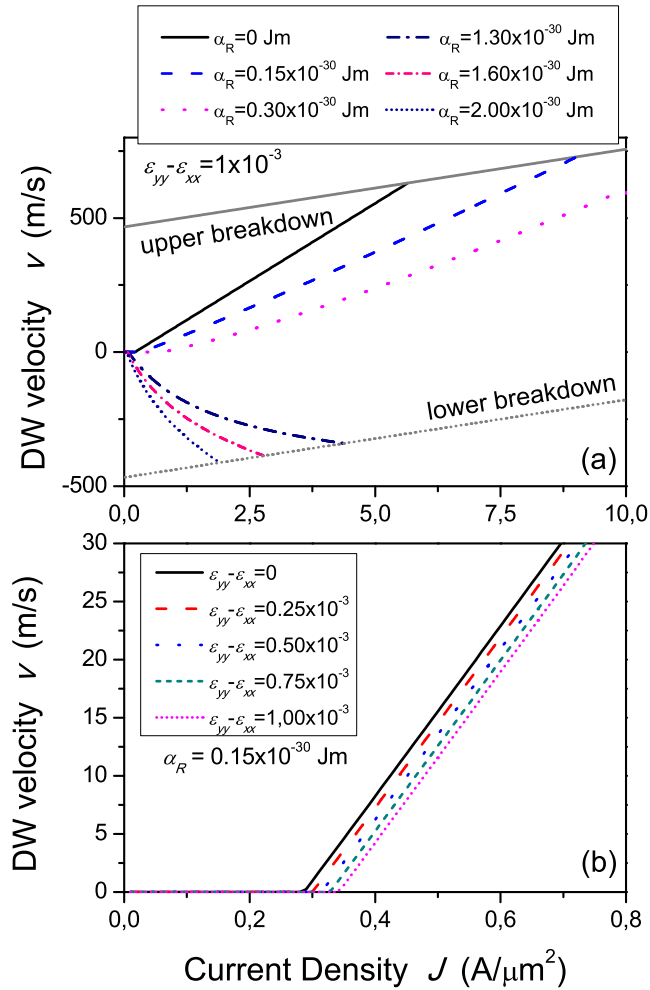
FIGURE 6. Steady DW velocity as a function of current density obtained by (a) fixing the piezo-strains and varying the Rashba parameter or (b) fixing the Rashba parameter and varying the piezo-strains.

FM layer and there exists a linear dependence between piezo-induced strains and the dry-friction coefficient. Moreover, in order to recover a Walker-like solution, the dimensionless coefficients $\widehat{\Gamma}$ and $\widetilde{\Gamma}$, directly related to the Rashba field, have been constrained to satisfy the conditions: $\left|\widehat{\Gamma}^2 - \widetilde{\Gamma}^2\right| < 1$ and $\left|\widetilde{\Gamma}\right|, \left|\widehat{\Gamma}\right| \simeq 0$.

Under such assumptions, an explicit expression for the steady DW velocity has been deduced. To the best of our knowledge, such an investigation has been so far undertaken via numerical tools only.

Our results have pointed out that the linearity between the DW velocity and the driving sources is preserved by dry friction and magnetoelastic contributions whereas a nonlinear behavior is induced by the Rashba effect. Moreover, it has been observed that the Rashba field acts as an additional degree of freedom which can be used to modify the DW mobility as well as the propagation direction. On the other hand, both Rashba and magnetoelastic fields have been found to affect the depinning threshold and the WB condition which delimit the steady regime.

Our results are also in qualitative agreement with numerical and experimental observations.

Acknowledgments

References

Allwood, D. A. (2005). "Magnetic Domain-Wall Logic". *Science* **309**(5741), 1688–1692. DOI: [10.1126/science.1108813](https://doi.org/10.1126/science.1108813).

Baltensperger, W. and Helman, J. S. (1993). "A model that gives rise to effective dry friction in micromagnetics". *Journal of Applied Physics* **73**(10), 6516–6518. DOI: [10.1063/1.352599](https://doi.org/10.1063/1.352599).

Baňas, L. (2008). "Adaptive techniques for Landau–Lifshitz–Gilbert equation with magnetostriction". *Journal of Computational and Applied Mathematics* **215**(2), 304–310. DOI: [10.1016/j.cam.2006.03.043](https://doi.org/10.1016/j.cam.2006.03.043).

Berger, L. (1984). "Exchange interaction between ferromagnetic domain wall and electric current in very thin metallic films". *Journal of Applied Physics* **55**(6), 1954–1956. DOI: [10.1063/1.333530](https://doi.org/10.1063/1.333530).

Boulle, O., Malinowski, G., and Kläui, M. (2011). "Current-induced domain wall motion in nanoscale ferromagnetic elements". *Materials Science and Engineering: R: Reports* **72**(9), 159–187. DOI: [10.1016/j.mser.2011.04.001](https://doi.org/10.1016/j.mser.2011.04.001).

Brandl, F., Franke, K., Lahtinen, T., Dijken, S. van, and Grundler, D. (2014). "Spin waves in CoFeB on ferroelectric domains combining spin mechanics and magnonics". *Solid State Communications* **198**, 13–17. DOI: [10.1016/j.ssc.2013.12.019](https://doi.org/10.1016/j.ssc.2013.12.019).

Bryan, M. T., Dean, J., and Allwood, D. A. (2012). "Dynamics of stress-induced domain wall motion". *Physical Review B* **85**(14). DOI: [10.1103/physrevb.85.144411](https://doi.org/10.1103/physrevb.85.144411).

Chen, D.-X., Pardo, E., and Sanchez, A. (2002). "Demagnetizing factors of rectangular prisms and ellipsoids". *IEEE Transactions on Magnetics* **38**(4), 1742–1752. DOI: [10.1109/tmag.2002.1017766](https://doi.org/10.1109/tmag.2002.1017766).

Consolo, G., Currò, C., Martinez, E., and Valenti, G. (2012). "Mathematical modeling and numerical simulation of domain wall motion in magnetic nanostrips with crystallographic defects". *Applied Mathematical Modelling* **36**(10), 4876–4886. DOI: [10.1016/j.apm.2011.12.024](https://doi.org/10.1016/j.apm.2011.12.024).

Consolo, G., Currò, C., and Valenti, G. (2014a). "Curved domain walls dynamics driven by magnetic field and electric current in hard ferromagnets". *Applied Mathematical Modelling* **38**(3), 1001–1010. DOI: [10.1016/j.apm.2013.07.032](https://doi.org/10.1016/j.apm.2013.07.032).

Consolo, G., Currò, C., and Valenti, G. (2014b). "Quantitative estimation of the spin-wave features supported by a spin-torque-driven magnetic waveguide". *Journal of Applied Physics* **116**(21), 213908. DOI: [10.1063/1.4903216](https://doi.org/10.1063/1.4903216).

Consolo, G. and Valenti, G. (2012). "Traveling Wave Solutions of the One-Dimensional Extended Landau-Lifshitz-Gilbert Equation with Nonlinear Dry and Viscous Dissipations". *Acta Applicandae Mathematicae*. DOI: [10.1007/s10440-012-9733-z](https://doi.org/10.1007/s10440-012-9733-z).

Consolo, G. and Valenti, G. (2017). "Analytical solution of the strain-controlled magnetic domain wall motion in bilayer piezoelectric/magnetostrictive nanostructures". *Journal of Applied Physics* **121**(4), 043903. DOI: 10.1063/1.4974534.

Gilbert, T. L. (1955). "A Lagrangian formulation of the gyromagnetic equation of the magnetization field". *Phys. Rev.* **100**, 1243.

Hu, J.-M., Yang, T., Momeni, K., Cheng, X., Chen, L., Lei, S., Zhang, S., Trolier-McKinstry, S., Gopalan, V., Carman, G. P., Nan, C.-W., and Chen, L.-Q. (2016). "Fast Magnetic Domain-Wall Motion in a Ring-Shaped Nanowire Driven by a Voltage". *Nano Letters* **16**(4), 2341–2348. DOI: 10.1021/acs.nanolett.5b05046.

Koyama, T., Chiba, D., Ueda, K., Kondou, K., Tanigawa, H., Fukami, S., Suzuki, T., Ohshima, N., Ishiwata, N., Nakatani, Y., Kobayashi, K., and Ono, T. (2011). "Observation of the intrinsic pinning of a magnetic domain wall in a ferromagnetic nanowire". *Nature Materials* **10**(3), 194–197. DOI: 10.1038/nmat2961.

Landau, L. D. and Lifschitz, E. M. (1935). "Zur Theorie der Dispersion der magnetische Permeabilitat der ferromafnetische Korpern". *Phys. Z. Sowjetunion* **8**, 158.

Lei, N., Devolder, T., Agnus, G., Aubert, P., Daniel, L., Kim, J.-V., Zhao, W., Trypiniotis, T., Cowburn, R. P., Chappert, C., Ravelosona, D., and Lecoeur, P. (2013). "Strain-controlled magnetic domain wall propagation in hybrid piezoelectric/ferromagnetic structures". *Nature Communications* **4**, 1378. DOI: 10.1038/ncomms2386.

Liang, C.-Y., Keller, S. M., Sepulveda, A. E., Bur, A., Sun, W.-Y., Wetzlar, K., and Carman, G. P. (2014). "Modeling of magnetoelastic nanostructures with a fully coupled mechanical-micromagnetic model". *Nanotechnology* **25**(43), 435701. DOI: 10.1088/0957-4484/25/43/435701.

Liu, L., Moriyama, T., Ralph, D. C., and Buhrman, R. A. (2011). "Spin-Torque Ferromagnetic Resonance Induced by the Spin Hall Effect". *Physical Review Letters* **106**(3). DOI: 10.1103/physrevlett.106.036601.

Liu, M., Obi, O., Cai, Z., Lou, J., Yang, G., Ziemer, K. S., and Sun, N. X. (2010). "Electrical tuning of magnetism in Fe_3O_4/PZN–PT multiferroic heterostructures derived by reactive magnetron sputtering". *Journal of Applied Physics* **107**(7), 073916. DOI: 10.1063/1.3354104.

Manchon, A., Koo, H. C., Nitta, J., Frolov, S. M., and Duine, R. A. (2015). "New perspectives for Rashba spin–orbit coupling". *Nature Materials* **14**(9), 871–882. DOI: 10.1038/nmat4360.

Martinez, E. and Finocchio, G. (2013). "Domain Wall Dynamics in Asymmetric Stacks: The Roles of Rashba Field and the Spin Hall Effect". *IEEE Transactions on Magnetics* **49**(7), 3105–3108. DOI: 10.1109/tmag.2013.2238899.

Mathurin, T., Giordano, S., Dusch, Y., Tiercelin, N., Pernod, P., and Preobrazhensky, V. (2016). "Stress-mediated magnetoelectric control of ferromagnetic domain wall position in multiferroic heterostructures". *Applied Physics Letters* **108**(8), 082401. DOI: 10.1063/1.4942388.

Mballa-Mballa, F. S., Hubert, O., He, S., Depeyre, S., and Meilland, P. (2014). "Micromagnetic Modeling of Magneto-Mechanical Behavior". *IEEE Transactions on Magnetics* **50**(4), 1–4. DOI: 10.1109/tmag.2013.2288911.

Miron, I. M., Moore, T., Szambolics, H., Buda-Prejbeanu, L. D., Auffret, S., Rodmacq, B., Pizzini, S., Vogel, J., Bonfim, M., Schuhl, A., and Gaudin, G. (2011). "Fast current-induced domain-wall motion controlled by the Rashba effect". *Nature Materials* **10**(6), 419–423. DOI: 10.1038/nmat3020.

Parkin, S. S. P., Hayashi, M., and Thomas, L. (2008). "Magnetic Domain-Wall Racetrack Memory". *Science* **320**(5873), 190–194. DOI: 10.1126/science.1145799.

Podio-Guidugli, P. and Tomassetti, G. (2002). "On the steady motions of a flat domain wall in a ferromagnet". *The European Physical Journal B* **26**(2), 191–198. DOI: 10.1140/epjb/e20020080.

Puliafito, V. and Consolo, G. (2012). "On the Travelling Wave Solution for the Current-Driven Steady Domain Wall Motion in Magnetic Nanostrips under the Influence of Rashba Field". *Advances in Condensed Matter Physics* **2012**, 1–8. DOI: 10.1155/2012/105253.

Pylypovskyi, O. V., Sheka, D. D., Kravchuk, V. P., Yershov, K. V., Makarov, D., and Gaididei, Y. (2016). "Rashba Torque Driven Domain Wall Motion in Magnetic Helices". *Scientific Reports* **6**(1). DOI: 10.1038/srep23316.

Ranieri, E. D., Roy, P. E., Fang, D., Vehsthedt, E. K., Irvine, A. C., Heiss, D., Casiraghi, A., Campion, R. P., Gallagher, B. L., Jungwirth, T., and Wunderlich, J. (2013). "Piezoelectric control of the mobility of a domain wall driven by adiabatic and non-adiabatic torques". *Nature Materials* **12**(9), 808–814. DOI: 10.1038/nmat3657.

Schryer, N. L. and Walker, L. R. (1974). "The motion of 180° domain walls in uniform dc magnetic fields". *Journal of Applied Physics* **45**(12), 5406–5421. DOI: 10.1063/1.1663252.

Shu, Y., Lin, M., and Wu, K. (2004). "Micromagnetic modeling of magnetostrictive materials under intrinsic stress". *Mechanics of Materials* **36**(10), 975–997. DOI: 10.1016/j.mechmat.2003.04.004.

Tatara, G., Kohno, H., Shibata, J., Lemaho, Y., and Lee, K.-J. (2007). "Spin Torque and Force due to Current for General Spin Textures". *Journal of the Physical Society of Japan* **76**(5), 054707. DOI: 10.1143/jpsj.76.054707.

Tatara, G., Takayama, T., Kohno, H., Shibata, J., Nakatani, Y., and Fukuyama, H. (2006). "Threshold Current of Domain Wall Motion under Extrinsic Pinning β-Term and Non-Adiabaticity". *Journal of the Physical Society of Japan* **75**(6), 064708. DOI: 10.1143/jpsj.75.064708.

Thiaville, A., Nakatani, Y., Miltat, J., and Suzuki, Y. (2005). "Micromagnetic understanding of current-driven domain wall motion in patterned nanowires". *Europhysics Letters (EPL)* **69**(6), 990–996. DOI: 10.1209/epl/i2004-10452-6.

Tiberkevich, V. and Slavin, A. (2007). "Nonlinear phenomenological model of magnetic dissipation for large precession angles: Generalization of the Gilbert model". *Physical Review B* **75**(1). DOI: 10.1103/physrevb.75.014440.

Wang, X. and Manchon, A. (2012). "Diffusive Spin Dynamics in Ferromagnetic Thin Films with a Rashba Interaction". *Physical Review Letters* **108**(11). DOI: 10.1103/physrevlett.108.117201.

Weiler, M., Brandlmaier, A., Geprägs, S., Althammer, M., Opel, M., Bihler, C., Huebl, H., Brandt, M. S., Gross, R., and Goennenwein, S. T. B. (2009). "Voltage controlled inversion of magnetic anisotropy in a ferromagnetic thin film at room temperature". *New Journal of Physics* **11**(1), 013021. DOI: 10.1088/1367-2630/11/1/013021.

Xu, Y., Yang, Y., Yao, K., Xu, B., and Wu, Y. (2016). "Self-current induced spin-orbit torque in FeMn/Pt multilayers". *Scientific Reports* **6**(1). DOI: 10.1038/srep26180.

Yamanouchi, M., Jander, A., Dhagat, P., Ikeda, S., Matsukura, F., and Ohno, H. (2011). "Domain Structure in CoFeB Thin Films With Perpendicular Magnetic Anisotropy". *IEEE Magnetics Letters* **2**, 3000304–3000304. DOI: 10.1109/lmag.2011.2159484.

Zhang, J. and Chen, L. (2005). "Phase-field microelasticity theory and micromagnetic simulations of domain structures in giant magnetostrictive materials". *Acta Materialia* **53**(9), 2845–2855. DOI: 10.1016/j.actamat.2005.03.002.

Zhang, S. and Li, Z. (2004). "Roles of Nonequilibrium Conduction Electrons on the Magnetization Dynamics of Ferromagnets". *Physical Review Letters* **93**(12). DOI: 10.1103/physrevlett.93.127204.

Zhu, B., Lo, C. C. H., Lee, S. J., and Jiles, D. C. (2001). "Micromagnetic modeling of the effects of stress on magnetic properties". *Journal of Applied Physics* **89**(11), 7009–7011. DOI: 10.1063/1.1363604.

Zighem, F., Faurie, D., Mercone, S., Belmeguenai, M., and Haddadi, H. (2013). "Voltage-induced strain control of the magnetic anisotropy in a Ni thin film on flexible substrate". *Journal of Applied Physics* **114**(7), 073902. DOI: 10.1063/1.4817645.

[a]   Università degli Studi di Messina,
     Dipartimento di Scienze Matematiche e Informatiche, Scienze Fisiche e Scienze della Terra,
     V.le F. Stagno D'Alcontres 31, 98166 Vill. S.Agata, Messina, Italy

[b]   Università degli Studi di Messina,
     Dipartimento di Ingegneria,
     C.da di Dio, 98166 Vill. S.Agata, Messina, Italy

[*]   To whom correspondence should be addressed | email: gvalenti@unime.it